Numerical comparison between two Spherical Harmonics Expansion models and a kinetic equation

J.P. Bourgade, A. Mellet and L. Mieussens

MIP, UMR 5640
Université Paul Sabatier, 118, route de Narbonne,
31062 Toulouse cedex, FRANCE

Abstract

In this paper, we investigate the reliability of two diffusion models, the SHE and coupled SHE models, by accurate numerical comparisons with a Boltzmann like equation. These models describe the transport of particles subject to collisions with the medium. Comparisons are given at three levels of description: at small times (transient regime), at the diffusion time (diffusion regime) and for long times (stationary regime). The three regimes are well described by both SHE models. A discussion of the main benefits and drawbacks of each of the SHE models is given, according to the regime

1 Introduction

With the development of microelectronics in the early 1950's, the description of the motion of electrons in semiconductors arose as a crucial problem. Kinetic models of Boltzmann type, though very accurate, proved to be computationaly expensive. On the other hand, macroscopic models such as Drift Diffusion become unrealistic as semiconductor components get miniaturized. Intermediate models have been recently proposed, such as the Spherical Harmonics Expansion (SHE) model which appears as a good compromise between physical accuracy and a low computational cost (see [1]). The SHE model is a diffusion type equation in the position-energy space for the particles distribution function. It takes the following form

$$N(\mathcal{E})\partial_t F(t,x,\mathcal{E}) - \tilde{\nabla}\cdot D(\mathcal{E})\tilde{\nabla}F(t,x,\mathcal{E}) = 0$$

where t denotes the time variable, x is the position and $\mathcal{E}$ is the (kinetic) energy of the particle. We note $N(\mathcal{E})$ the density of states, $F(t,x,\mathcal{E})$ is the density of particles at time t, located at x, evolving with a kinetic energy $\mathcal{E}$. The energy dependent diffusion

tensor $D(\mathcal{E})$ is a positive tensor and $\tilde{\nabla} = \nabla_x + E(\partial/\partial\mathcal{E})$, where E is a force field applied to the particles, is a generalized gradient in the position-energy space. Such a model can be derived from kinetic models under the assumption of dominant elastic scattering between the particles and the medium. Nevertheless, inelastic regimes are quite frequent and a natural problem is to extend the (theoretical) reliability of SHE models to thermalizations due to inelastic scatterings. The work on such regimes was initiated by P. Degond in [2] and led to the introduction of coupled SHE models which can be written as follows

$$N(\mathcal{E})\partial_t F(t,x,\mathcal{E}) - \tilde{\nabla} \cdot \int_{\mathcal{E}'>0} D_\alpha(\mathcal{E}',\mathcal{E})\tilde{\nabla}F(t,x,\mathcal{E}')d\mathcal{E}' = 0.$$

In this case, the diffusion tensor D_α is non local. The model is 'coupled' in the sense that the current of particles at a given energy depends on the distribution of particles at any energy, thus coupling different levels of energy. Indeed, introducing the current of particles J, the coupled SHE model can also be written

$$N(\mathcal{E})\partial_t F(t,x,\mathcal{E}) + \tilde{\nabla} \cdot J(t,x,\mathcal{E}) = 0, \quad J(t,x,\mathcal{E}) = -\int_{\mathcal{E}'>0} D_\alpha(\mathcal{E}',\mathcal{E})\tilde{\nabla}F(t,x,\mathcal{E}')d\mathcal{E}'$$

where the first equation is nothing but a conservation law while the second one takes the form of a Fourier law relating the current of particles to the (generalized) gradient of the density of particles. One can easily see the non local influence of the gradient of F on the value of the current at a given energy $\mathcal{E}$. The diffusion tensor depends on a parameter α which controls the coupling between energy levels. For $\alpha = 0$, the coupled SHE model degenerates into a classical uncoupled SHE model. The theoretical derivation of the coupled SHE model can be performed for a limited range of values for α ($0 \leq \alpha < 1/2$ in our case). One of the aims of this work is to study the influence of this parameter on the reliability of the coupled SHE model.

More generally, we aim at assessing the reliability of both the coupled and the uncoupled SHE models by comparing them to the kinetic model of Boltzmann type from which they can be derived. As a first step, we propose monodimensional simulations in both space and velocity in a force free case. In this case, we do not expect the SHE models to be computationaly less expensive than the kinetic model since the number of variables is the same in both models (the 1D velocity variable is changed for a 1D energy variable in the case of the SHE models). However, this simple framework enables us to make a rather exhaustive comparison between the models. The introduction of a self consistent electric field (which represents a

wide range of semiconductor applications) and computations in higher dimensions in the phase space are postponed to future work. Up to our knowledge, the only existing systematic comparison between the SHE model and a kinetic model is made a stationary case [3] and deals only with the uncoupled SHE model. In the present work, we propose a general study not only of the SHE model but also of the coupled SHE model, and the comparisons are performed in small and diffusion times as well as in stationary regimes.

The paper is organized as follows. In section 2 we introduce the different models: the kinetic one and the SHE models. Next, section 3 is dedicated to the discretization of these models. In section 4, the test case is precisely described. This section also gathers the different numerical results: while section 4.1 is devoted to the study of the diffusion and stationary regimes, we give the analysis of the theoretically worst situation for the SHE model, the transient regime, in section 4.2.

2 The microscopic model and the SHE models

In this section, we introduce the microscopic model which will be the basis of the comparisons. We also present the macroscopic SHE models and their derivation starting from the kinetic model.

2.1 The kinetic model

We consider a set of particles as described by a distribution function $f = f(t, x, v)$. The quantity $f(t, x, v)dxdv$ represents the number of particles at time t in an elementary volume $dxdv$ in the phase space around (x, v). The function f depends on time t, position x and velocity v, and is defined on $(0, \infty) \times (0, L) \times \mathbb{R}$. Its evolution is described by a kinetic equation supplemented with initial and boundary conditions. On the left boundary, an inflow of particles is modeled by a Dirichlet condition f_l for positive velocities. On the right boundary, outgoing particles are reemitted in the domain according to a specular reflexion on the wall. The initial condition is assumed to be equal to zero: $f(0, x, v) = 0$. The model reads

$$\begin{aligned}
&\partial_t f + v\partial_x f = Q(f), && x \in (0,L),\ v \in \mathbb{R},\ t \in (0,\infty),\\
&f(0,x,v) = 0, && x \in (0,L),\ v \in \mathbb{R},\\
&f(t,0,v) = f_l(v), && v > 0,\ t \in (0,\infty),\\
&f(t,L,v) = f(t,L,-v), && v < 0,\ t \in (0,\infty).
\end{aligned} \tag{1}$$

Since we want to investigate the relevance of the SHE model even when inelastic mechanisms are dominant, we define the collision operator by

$$Q(f) = (1-\beta)Q^0_{el}(f) + \beta Q_{in}(f), \tag{2}$$

where the parameter β lies in $[0,1]$. The operator Q^0_{el} is given by

$$Q^0_{el}(f) = \nu\big([f](v) - f(v)\big), \tag{3}$$

where $[f](v)$ denotes the average of f on a constant energy surface, which, in this one-dimension framework, is given by $[f](v) = (f(v) + f(-v))/2$, and ν denotes the constant collision frequency. This operator is elastic in the sense that it does not change the number of particles on a shell of constant energy (it does not act on f through the modulus of the velocity). The operator Q_{in} is said to be inelastic and is written

$$Q_{in}(f) = \nu\left(\int_{\mathbb{R}} f(v')\,dv'\,M(\mathcal{E}(v)) - f(v)\right), \tag{4}$$

where $M(\mathcal{E}) = C\exp(-\mathcal{E}/(kT))$ denotes the maxwellian distribution of particles of kinetic energy $\mathcal{E}$ and C is a constant such that $\int_{\mathbb{R}} M(\mathcal{E}(v))dv = 1$. We denote by $\mathcal{E}(v) = m^*v^2/2$ the kinetic energy of particles of mass m^*.

In order to derive the macroscopic SHE models, we introduce the following rescaled variables:

$$x' = \varepsilon x, \quad t' = \varepsilon^2 t$$

where ε is a small parameter. We also introduce λ such that $L = \lambda/\varepsilon$ and τ such that $T_{diff} = \tau/\varepsilon^2$ is the diffusion time. Then, the rescaled distribution function f^ε is solution to:

$$\begin{aligned}
&\partial_{t'} f^\varepsilon + \frac{1}{\varepsilon} v\partial_{x'} f^\varepsilon = \frac{1}{\varepsilon^2} Q(f^\varepsilon) && x' \in (0,\lambda),\ v \in \mathbb{R},\ t' \in (0,\infty),\\
&f^\varepsilon(0,x',v) = 0, && x' \in (0,\lambda),\ v \in \mathbb{R},\\
&f^\varepsilon(t',0,v) = f_l(v), && v > 0,\ t' \in (0,\infty),\\
&f^\varepsilon(t',\lambda,v) = f^\varepsilon(t',\lambda,-v), && v < 0,\ t' \in (0,\infty).
\end{aligned} \tag{5}$$

In the next section, we detail the macroscopic models obtained by investigating the behaviour of f^ε as ε goes to zero.

2.2 The standard SHE model

We start from the rescaled equation (5). To obtain the SHE model, the inelastic collision operator (4) is split as follows:

$$\begin{aligned} Q_{in}(f) &= \nu\big([f](v) - f(v)\big) + \nu\left(\int_{\mathbb{R}} f(v')\,dv' M(\mathcal{E}(v)) - [f](v)\right) \\ &= Q^0_{el}(f) + Q^0_{in}(f). \end{aligned} \tag{6}$$

We suppose that β is of order ε^2 and introduce $\beta = \varepsilon^2\tilde{\beta}$. Consequently, the collision operator $Q(f)$ is written

$$Q(f) = Q^0_{el}(f) + \varepsilon^2\tilde{\beta}Q^0_{in}(f)\,,$$

and we expect the SHE model to furnish a good approximation of the Boltzmann equation (1) when $\tilde{\beta}$ is of order 1. More precisely, we have

Proposition 2.1 *The solution f^ε of the system of equations (5) is such that we (formally) have $f^\varepsilon = F + \varepsilon f^1 + \mathcal{O}(\varepsilon^2)$, with*

$$f^1 = -\frac{v}{\nu}\partial_x F$$

and where $F = F(t,x,\mathcal{E})$ is the solution of the following SHE set of equations (written in kinetic variables)

$$\begin{aligned} &\partial_t F - D\partial_x^2 F = \nu\beta\left(\int_{\mathbb{R}} F(\mathcal{E}(v'))dv'\,M(\mathcal{E}(v)) - F\right), x \in (0,L), t \in (0,\infty), v \in \mathbb{R}, \\ &F(0,x,\mathcal{E}) = 0, \quad \mathcal{E} \in (0,\infty) \\ &F(t,0,\mathcal{E}(v)) - \Lambda\partial_x F(t,0,\mathcal{E}(v)) = f_l(v), \quad v > 0 \\ &\partial_x F(t,L,\mathcal{E}) = 0, \quad \mathcal{E} \in (0,\infty). \end{aligned}$$

The diffusion tensor D is defined by $D = |v|^2/\nu$ and the extrapolation length arising in the Robin condition is $\Lambda = \frac{|v|}{\nu}$.

In addition, the velocity average of f^ε and the density and the energy associated to the distribution f^ε are approximated up to second order by the corresponding quantities given by F. That is:

$$\begin{aligned} &[f^\varepsilon] = F + \mathcal{O}(\varepsilon^2) \\ &\int_{\mathbb{R}} f^\varepsilon(t,x,v)dv = \int_{\mathbb{R}} F(t,x,\mathcal{E}(v))dv + \mathcal{O}(\varepsilon^2) \\ &\int_{\mathbb{R}} \mathcal{E}(v) f^\varepsilon(t,x,v)dv = \int_{\mathbb{R}} \mathcal{E}(v)F(t,x,\mathcal{E}(v))dv + \mathcal{O}(\varepsilon^2). \end{aligned}$$

Proof: The formal proof of this proposition is similar, though simpler, to the proof of proposition 2.2, which is given in section 2.3. □

2.3 The coupled SHE model

The derivation of a model which would take into account the coupling between the flux and the density at different energy levels is more recent. It first appeared in [2]. See also [4] for an application to the neutronics, and [5] in the case of electron-phonon interactions in semiconductor devices. It relies on the combination of two splittings of the inelastic operator. A first splitting is given in (6) and will be refered to as the 'local' splitting because the elastic part Q^0_{el} acts on f only through the sign of the velocity and not on the kinetic energy. Now we introduce a 'non local' splitting in the sense that its elastic part Q^1_{el} acts on f through the energy too (it involves an integration with respect to v):

$$\begin{aligned} Q_{in}(f) &= \nu M(\mathcal{E}(v)) \left(\int_{\mathbb{R}} f(v')\, dv' - 2 \int_0^\infty f(\mathrm{sign}(v)v') dv' \right) \\ &\quad + \nu \left(2 \int_0^\infty f(\mathrm{sign}(v)v') dv'\, M(\mathcal{E}(v)) - f(v) \right) \\ &= Q^1_{el}(f) + Q^1_{in}(f)\,, \end{aligned} \tag{7}$$

where $\mathrm{sign}(v) = \pm 1$ when $\pm v > 0$.

Following [2], we consider the convex combination $Q_{in} = (1-\alpha)\,(Q^0_{el} + Q^0_{in}) + \alpha\,(Q^1_{el} + Q^1_{in})$ of the two splittings (6) and (7). Introducing this combination in (2), we find

$$Q = (1-\alpha\beta)Q^0_{el} + \alpha\beta Q^1_{el} + \beta((1-\alpha)Q^0_{in} + \alpha Q^1_{in})\,.$$

Based on the work [2], the following proposition holds

Proposition 2.2 *If $\alpha\beta < 1/2$, then the solution f^ε of equations (5) is such that we (formally) have $f^\varepsilon = F + \varepsilon f^1 + \mathcal{O}(\varepsilon^2)$, with*

$$f^1 = \int \chi(w,v) \partial_x F\,(t,x,\mathcal{E}(w))\, dw$$

and where $F = F(t,x,\mathcal{E})$ is the solution of the following coupled SHE system of

equations (written in kinetic variables):

$$\partial_t F + \partial_x J = \nu\beta \left(\int_{\mathbb{R}} F(\mathcal{E}(w))dw\, M(\mathcal{E}(v)) - F(\mathcal{E}(v)) \right) \tag{8}$$

$$J(\mathcal{E}(v)) = -D_{\alpha\beta}(v)\partial_x F(\mathcal{E}(v)) - \int_{\mathbb{R}} \Delta_{\alpha\beta}(v,w)\partial_x F(\mathcal{E}(w))\, dw\,, \tag{9}$$

$$F(0,x,\mathcal{E}(v)) = 0$$

$$F(t,0,\mathcal{E}(v)) + \int \chi(v,w)\partial_x F(t,0,\mathcal{E}(w))dw = f_l(v), \quad v > 0 \tag{10}$$

$$\int \chi(v,w)\partial_x F(t,L,\mathcal{E}(w))dw = 0 \tag{11}$$

with $x \in (0,L)$, $t \in (0,\infty)$, *and:*

$$D_{\alpha\beta}(v) = \frac{|v|^2}{\nu(1-\alpha\beta)}, \qquad \Delta_{\alpha\beta}(v,w) = \frac{\alpha\beta}{\nu(1-\alpha\beta)} M(\mathcal{E}(v))|v||w|.$$

At last, $\chi(w,v) = \overline{\chi}(w,v) + \theta(w,v)$, *where*

$$\overline{\chi}(w,v) = -\frac{1}{\nu(1-\alpha\beta)}\frac{v}{2}\delta(\mathcal{E}(w)-\mathcal{E}(v)), \quad \theta(w,v) = -\frac{\alpha\beta}{\nu(1-\alpha\beta)} M(\mathcal{E}(v))sign(v)|w|. \tag{12}$$

Proof: This proof is only formal. The convergence of f^ε to F has been rigorously established in [2] in an unbounded domain, without boundary conditions. A formal approximation result is proven in [6] for the uncoupled SHE model with boundary conditions. The rigorous proof of this approximation problem remains an open question.

As a preliminary, we underline that, if $\alpha\beta < 1/2$, then the null space $N(Q^\alpha_{el})$ of the operator $Q^\alpha_{el} = (1-\alpha\beta)Q^0_{el} + \alpha\beta Q^1_{el}$ is the set of functions depending on v only through the energy $\mathcal{E}(v)$. In addition, the equation

$$Q^\alpha_{el}(f) = g \tag{13}$$

of unknown f can be solved if g belongs to the range of Q^α_{el} in $L^2(\mathbb{R}_v; M^{-1}dv)$. It is straightforward to prove that, in our case, this condition reads:

$$[g] = \frac{1}{2}\left(g(v) + g(-v)\right) = 0. \tag{14}$$

Moreover, under condition (14), the solution f of equation (13) is unique in the class of functions h such that $[h] = 0$.

We consider the following formal Hilbert expansion of f^ε in powers of ε: $f^\varepsilon = f^0+\varepsilon f^1+\varepsilon^2 f^2+\varepsilon^3 f^3+r^\varepsilon$. Inserting this expansion in equation (5) we get, as $\varepsilon \to 0$, $Q^\alpha_{el}(f^0) = 0$, which implies that $f^0(t,x,v)$ is a function of the energy only, denoted by $F = F(t,x,\mathcal{E}(v))$. Now, if we consider terms of order ε in the expansion, we get the following relation between F and f^1

$$Q^\alpha_{el}(f^1) = v\,\partial_x F.$$

Note that, by oddness, $v\partial_x F$ satisfies the solvability condition (14). It can be proved that a solution of this equation is

$$f^1(t,x,v) = \int \chi(w,v)\partial_x F(t,x,\mathcal{E}(w))dw$$

where χ is given by (12). Then the current $J = [vf^1]$ takes the expected form (9).

Considering second order terms in (5) yields

$$\partial_t f^0 + v\partial_x f^1 = Q^\alpha_{el}(f^2) + \tilde{\beta} Q^\alpha_{in}(f^0).$$

Straightforward computations (that are detailed in [2]) show that the solvability condition for this equation of unknown f^2 corresponds to equation (8). Note that, in our case, f^2 can be chosen identically equal to zero.

We now turn our attention to the derivation of the boundary conditions. Our aim is to prove that the conditions (10), (11) are necessary to get an accurate enough approximation of the kinetic equation by the SHE model. For this sake, the remainder r^ε in the Hilbert expansion has to be estimated. We first establish an equation solved by r^ε.

Considering order ε^3 terms in (5), we get $Q^\alpha_{el}(f^3) = \partial_t f^1 - \tilde{\beta} Q^\alpha_{in}(f^1)$ (since $f^2 = 0$). The solvability condition (14) for this equation is satisfied according to the explicit form obtained for f^1 and to conservation properties of the collision operator. Consequently, f^3 exists.

If we come back to the rescaled variables (t', x', v) (but dropping the primes for the sake of clarity), we see that $r^\varepsilon(t,x,v)$ is solution of

$$\partial_t r^\varepsilon + \frac{1}{\varepsilon} v\partial_x r^\varepsilon = \frac{1}{\varepsilon^2} Q^\alpha_{el}(r^\varepsilon) + \tilde{\beta} Q^\alpha_{in}(r^\varepsilon) + \varepsilon^2 S^\varepsilon(t,x,v)\,, \tag{15}$$

where the source term $S^\varepsilon(t,x,v)$ is bounded with respect to ε.

In order to prove that we get a second order approximation of f^ε, we need to investigate the boundary values of r^ε. Along the boundary $x = 0$ and for $v > 0$, we have $f^\varepsilon(t, 0, v) = f_l(v)$. It implies for r^ε

$$r^\varepsilon(t, 0, v) = f_l(v) - F(t, 0, \mathcal{E}(v)) - \varepsilon \int \chi(w, v)\partial_x F(t, 0, \mathcal{E}(w))dw - \varepsilon^3 f^3(t, 0, v)$$

Note that this equation is still written in rescaled variables. To get a second order approximation, F must be chosen such that

$$F(t, 0, \mathcal{E}(v)) + \varepsilon \int \chi(w, v)\partial_x F(t, 0, \mathcal{E}(w)dw = f_l(v)$$

which, in macroscopic variables, is exactly the Robin condition (10). Note that taking a Dirichlet condition would lead to a first order approximation only.

On the other hand, along the boundary $x = L$, and for $v < 0$, we have $f^\varepsilon(t, \lambda, v) - f^\varepsilon(t, \lambda, -v) = 0$. It implies for r^ε (still in rescaled variables):

$$\begin{aligned} r^\varepsilon(t, \lambda, v) - r^\varepsilon(t, \lambda, -v) &= -2\varepsilon \int \chi(w, v)\partial_x F(t, \lambda, \mathcal{E}(w))dw + \mathcal{O}(\varepsilon^3) \\ &= \mathcal{O}(\varepsilon^3) \end{aligned}$$

if we assume (11).

Therefore, the approximation is globally of second order with respect to ε as soon as the boundary conditions are chosen to be (10) and (11). Indeed, r^ε is, up to second order terms, the solution of a linear kinetic equation with homogeneous boundary conditions and an initial condition equal to zero.

It should be noted that no boundary layer corrector is needed in this case (contrary to SHE or Drift Difusion models in several dimensions). □

3 Numerical methods

In this section, we present the numerical methods used in our computations. From now on we consider a bounded velocity domain $(-V_{max}, V_{max})$. The numerical value of V_{max} is to be precised in section 4.

3.1 The discretized Boltzmann equation

We deal with equation (1), where the collision operator is defined by (2), (3) and (4). Then, the kinetic equation takes the following form:

$$\partial_t f + v\partial_x f = \nu \left[(1-\beta)\frac{f(-v)-f(v)}{2} + \beta \left(\int_{\mathbb{R}} f(v')dv' M(\mathcal{E}(v)) - f(v) \right) \right]. \quad (1)$$

Let $x_i = i\Delta x$, $v_j = (j - j_{max})\Delta v$ and $t_n = n\Delta t$ denote the mesh respectively on $[0, L]$, $[-V_{max}, V_{max}]$, and $[0, T_{max}]$, with $i \in [\![0, i_{max}]\!]$, $j \in [\![0, 2j_{max}]\!]$ and $n \in [\![0, n_{max}]\!]$.

The solution of equation (1) is assumed to be approximated at each point of the grid by $f_{i,j}^n \approx f(t_n, x_i, v_j)$. Note that $f(t_n, x_i, -v_j)$ is approximated by $f_{i,2j_{max}-j}^n$. The sequence $f_{i,j}^n$ is constructed by a second order scheme in space and time. The second order approximation in time is obtained thanks to the classical Strang splitting.

1. Solve
$$\left\{ \begin{array}{rcl} \partial_t g_1 + \partial_x g_1 & = & 0 \\ g_{1|t=0} & = & f_{i,j}^n \end{array} \right. \quad (2)$$
and set $f_{i,j}^{n+1/3} = g_1\left(\frac{\Delta t}{2}, x_i, v_j\right)$ (or a second order approximation of $g_1\left(\frac{\Delta t}{2}\right)$).

2. Solve
$$\left\{ \begin{array}{rcl} \partial_t g_2 & = & Q(g_2) \\ g_{2|t=0} & = & f_{i,j}^{n+1/3} \end{array} \right. \quad (3)$$
and set $f_{i,j}^{n+2/3} = g_2(\Delta t, x_i, v_j)$ (or a second order approximation of $g_2(\Delta t)$).

3. Solve
$$\left\{ \begin{array}{rcl} \partial_t g_3 + \partial_x g_3 & = & 0 \\ g_{3|t=0} & = & f_{i,j}^{n+2/3} \end{array} \right.$$
and set $f_{i,j}^{n+1} = g_3\left(\frac{\Delta t}{2}, x_i, v_j\right)$ (or a second order approximation of $g_3\left(\frac{\Delta t}{2}\right)$).

We now describe the numerical solving of each step.

First and third steps: the transport equation.

We use the semi-lagrangian method that we briefly describe hereafter (see [7] for a detailed presentation). We remark that equation (2) can be solved thanks to a characteristic method. Precisely, if we assume that the solution is known on any mesh point (x_i, v_j) at time t^{n-1}, then at the next time step t_n it satisfies

$$f(t^n, x_i, v_j) = f(t^{n-1}, X(t^{n-1}, t^n, x_i, v_j), v_j),$$

where $X(t,s,x,v)$ denotes the solution at time t of the ordinary differential equation associated to the characteristic curve that represents the trajectory of a particle of velocity v located in x at time s (when no collision occur). Namely, $X(t^{n-1},t^n,x_i,v_j) = x_i - v_j\Delta t$. The only problem is that the ending point $X(t^{n-1},t^n,x_i,v_j)$ of the characteristic curve is generally not a mesh point. Therefore, we have to approximate the value of $f(t^{n-1},X(t^{n-1},t^n,x_i,v_j),v_j)$ by interpolation. In order to keep a second order approximation, we use a third order Lagrange interpolation (a second order interpolation would be sufficient but we follow [8] and use an interpolation of odd order for the scheme to be centered).

Second step: the collision equation.

The approximate solution $f_{i,j}^{n+1/3}$ of the free transport equation (2) is known at time t_n and for all i, j. We obtain the approximated solution $f_{i,j}^{n+2/3}$ by solving the ordinary differential equation (3) by the mid-point formula

$$f^{n+2/3} = f^{n+1/3} + \Delta t\, Q\left(f^{n+1/3} + \frac{\Delta t}{2} Q\left(f^{n+1/3}\right)\right).$$

3.2 The SHE models

As long as there is no force field, the SHE model is nothing but a diffusion equation with respect to the position variable, with a source term mixing the energy levels. We can write it as follows:

$$\partial_t F(t,x,\mathcal{E}) - D(\mathcal{E})\partial_{xx}^2 F(t,x,\mathcal{E}) + \nu\beta F(t,x,\mathcal{E}) = \nu\beta\rho(t,x)M(\mathcal{E}), \tag{4}$$

where $\rho(t,x) = \int F(t,x,\mathcal{E})\frac{d\mathcal{E}}{2\sqrt{\mathcal{E}}}$ is the density associated to F. In order to avoid numerical difficulties due to the stiff jacobian $1/\sqrt{\mathcal{E}}$, we prefer to compute the density by using the following equivalent expression

$$\rho(t,x) = \int_{\mathbb{R}} F(t,x,\mathcal{E}(v))dv.$$

In the left-hand side of (4), the variable v is nothing but a parameter. We shall therefore discretize (4) on $[0,L]\times[0,V_{max}]$ using a classical Cranck-Nicolson scheme. The gain term of the collision operator is kept explicit. Using the same space grid as for the Boltzmann equation and the velocity grid $v_j = j\Delta v, j \in [\![0, j_{max}]\!]$, equation

(4) is then discretized by

$$\frac{F_{i,j}^{n+1}-F_{i,j}^{n}}{\Delta t}-D(\mathcal{E}(v_j))\left(\frac{1}{2}\delta_x^2F_{i,j}^{n+1}+\frac{1}{2}\delta_x^2F_{i,j}^{n}\right)\\ +\nu\beta\left(\frac{1}{2}F_{i,j}^{n+1}+\frac{1}{2}F_{i,j}^{n}\right)=\nu\beta\rho_i^nM(\mathcal{E}(v_j))\,,$$

with $\rho_i^n=\sum_{j=0}^{j_{max}-1}\left(F_{i,j}^n+F_{i,j+1}^n\right)\Delta v$, and $\delta_x^2F_{i,j}=\dfrac{F_{i+1,j}-2F_{i,j}+F_{i-1,j}}{\Delta x^2}$. The boundary conditions are also discretized in a semi-implicit way.

Note that, due to the explicit gain term, the Cranck-Nicolson scheme is a first order scheme in time, but a second order scheme in space and is unconditionnally stable.

We shall discretize the coupled SHE model in the same way, keeping explicit the coupling terms coming from the current equation. We get:

$$\frac{F_{i,j}^{n+1}-F_{i,j}^{n}}{\Delta t}-D_{\alpha\beta}(v_j)\left(\frac{1}{2}\delta_x^2F_{i,j}^{n+1}+\frac{1}{2}\delta_x^2F_{i,j}^{n}\right)\\ +\nu\beta\left(\frac{1}{2}F_{i,j}^{n+1}+\frac{1}{2}F_{i,j}^{n}\right)=\nu\beta\rho_i^nM(v_j)+\Phi_{i,j}^n\,, \tag{5}$$

with

$$\Phi_{i,j}^n=\sum_{k=0}^{M-1}\left(\Delta_{\alpha\beta}(v_j,v_k)\delta_x^2F_{i,k}^n+\Delta_\alpha(v_j,v_{k+1})\delta_x^2F_{i,k+1}^n\right)\Delta v\,.$$

4 Numerical results

We consider the evolution of an inflow of electrons in an interval $(0,L)$. The electron mass is taken equal to $m^*=9.010\times10^{-31}kg$ and we assume that the surrounding medium is at a fixed temperature $\Theta=300K$. The Boltzmann constant is $k_B=1.38054\times10^{-23}\,J.K^{-1}$ and we suppose that the collision frequency is $\nu=10^{12}s^{-1}$. The typical microscopic time is given by $\tau=\nu^{-1}$ and the typical microscopic length is $\lambda=V_{th}\tau$, where the thermal velocity of the cloud of electrons can be computed according to the formula $V_{th}=\sqrt{k_B\Theta/m^*}$. We have $\tau=10^{-12}s$ and $\lambda=10^{-7}m$. The length of the domain is $L=V_{th}/(\nu\varepsilon)$, the velocity domain is $(-V_{max},V_{max})$, with $V_{max}=3\sqrt{2}V_{th}=287\,806\,ms^{-1}$. At last, the diffusion time is defined as $T_{diff}=1/(\nu\varepsilon^2)$.

At the beginning ($t = 0$), no particle is present in the interval $(0, L)$. On the left boundary ($x = 0$) particles are injected according to a narrow normalized Maxwellian distribution centered on the velocity $V_{max}/2$ and of temperature $m^*(V_{max}/50)^2/k_B = 18\Theta/(50^2)$. This Maxwellian is normalized on $(-V_{max}, V_{max})$ and we note C the normalization constant. On the right boundary, particles undergo a specular reflection. The initial and boundary conditions read

$$\begin{aligned} f_I(x,v) &= 0 \quad \forall\, x \in (0,L),\ \forall\, v \in (-V_{max}, V_{max}), \\ f(t,0,v) &= f_l(v) = C \exp\left(-\frac{m^*(V_{max}/2 - v)^2}{2k_B\Theta}\right), \forall\, v \in (0,\ V_{max})\, \forall\, t > 0, \\ f(t,L,v) &= f(t,L,-v) \quad \forall\, v \in (-V_{max}, 0)\ \forall\, t > 0. \end{aligned}$$

The simulations were performed with 2×50 steps in velocity (or 50 steps in energy for the SHE models), 100 steps in space, and a time step of $2{\times}10^{-16}$s. Due to the left boundary condition, a small time step has to be taken in the kinetic model for reasons of precision of the lagrangian method (we postpone the analysis of this phenomenon to future work). Nevertheless, a study of convergence has been performed and the space, velocity and time steps used in the simulations presented in this paper were taken optimals. Namely, dividing the space and velocity steps by 2 leads to no meaningful difference, and the same is observed if we divide the optimal time step by 10.

First, we present a qualitative comparison between the coupled SHE model and the kinetic model. A 3D representation of the distribution function depending on space and velocity is presented at different times. Note that the distribution function is not directly given by the SHE models (since the solutions of the SHE models are even with respect to the velocity). In this comparison, the approximated distribution function is obtained by adding the distribution F described by the SHE model and the first order corrector f^1 (see propositions 2.1 and 2.2).

The aim is to show how the diffusion model is able to give some information on the global behaviour of the cloud of particles. The comparison is given for $\varepsilon = 0.1$, $\beta = 0.3$, $\alpha = 0.166$, that is for a situation near the diffusion regime, but with rather inelastic collisions (we recall that the SHE models are derived theoretically for values of β close to ε^2).

At the beginning of the simulation ($T = 0.001T_{diff}$, see Fig. 1) almost no particle is in the domain. The inflow of particles on nonnegative velocities can be seen at its very beginning and appears as a rough peak on the kinetic simulation.

At this time, the approximation by the SHE model is qualitatively bad: a negative peak appears for negative velocities. Moreover, as any diffusion model, the SHE model involves propagation phenomena with infinite velocity. This is well seen on Fig. 1: the peak for positive velocities is not as thin as for the kinetic model in the position direction. Even in a very short time period, the number of particles is not null in the domain (while it is null for the kinetic model). Nevertheless, as the following figures show, this drawback has no major influence on the qualitative behaviour for longer times.

The two following figures show the evolution of the incoming particles: due to elastic collisions, the distribution is somewhat symmetrized in velocity (a small peak appears for negative velocities) while inelastic collisions tend to relax the distribution function of particles towards a Maxwellian (see Fig. 2). Nevertheless, the distribution function cannot relax completely to a Maxwellian because of the incoming boundary condition on the left. The propagation of the incoming particles throughout the domain is well seen and Fig. 2 shows the reflection on the right boundary. The time at which the inflow hits the right boundary and undergoes the specular reflexion is $0.05T_{diff}$ in the kinetic case and this bounce is well seen on the SHE simulation at about the same time: Fig. 2 shows a rough increase in the number of particles leaving the right boundary with a negative velocity. The bounce is particularly clear for $v = V_{max}/2$, the velocity corresponding to the incoming particles (the peak on positive velocities). It is an important point that the coupled SHE model is able to show this bounce at the same time as the kinetic model does. Note that we are still in a transient regime, where the diffusion model was not expected to be relevant. Figure 3 shows the propagation of these reflected particles towards the left boundary. Since there is no boundary condition on the left for particles with a negative velocity, these particles go out of the domain without affecting the distribution function. At this step, the evolution of the cloud of particles becomes quite simple: the centered hump keeps on growing towards an equilibrium which is approximately reached for $T = 5T_{diff}$. Figure 4 shows the distribution function at $10T_{diff}$, *i.e.* in the stationary regime. Again, the kinetic and coupled SHE models coincide as far as the qualitative behaviour is concerned. A more precise analysis is given in the following section.

4.1 The diffusion and stationary regimes

From a theoretical point of view, diffusion models are supposed to behave correctly not only in stationary regimes but also in diffusion regimes, that is for large scales in space and for such long times that the scattering phenomena have been numerous enough for the distribution function to be close to an equilibrium of the kinetic collision operator. In our case, this means that there is reasonable hope for the SHE models to be reliable for times near T_{diff}. In the case of SHE models, it has already been observed that they indeed give results very close to those obtained thanks to kinetic models of Boltzmann type in stationary regimes, at least in the case of applications to plasma physics (see [3]).

In all the figures to follow in this section, regarding the density, the energy or the distribution function, the kinetic model is pictured by a continuous line, the SHE model by a dotted line and the coupled SHE model by a dashed line.

First, we present a comparison in the most suitable situation: at T_{diff}, for $\varepsilon = 0.1$, we take $\beta = 0.01 = \varepsilon^2$. In this case, the SHE models are expected to give their best. Indeed, as can be seen in Fig. 5, the macroscopic density and energy computed by means of the kinetic model are well approached by both SHE models.

But, not only macroscopic quantities are well described by these models. The distribution function of particles, as given by the kinetic model, can be approximated by using the first order correction term in the Hilbert expansion as seen in the proof of proposition 2.2. Figure 6 shows that this approximation is very accurate. This figure presents a section of the distribution function at a fixed position ($x = L/2$) for any value of the velocity. Note that the peaks are approached very accurately by both models. The distribution function is not even with respect to the velocity because of the dissymmetry of the left boundary condition: the peak for negative velocities is smaller than the other one. Nevertheless, even though the solutions of the SHE systems of equations are even with respect to the velocity, considering the first order corrector allows to recover the shape of the distribution.

Computations can be carried on until the steady state is reached, which, in our case, is the case at approximately $T = 5T_{diff}$. Here again, in Fig. 7 we present the density and the energy. The density is still very well approached while the energy is less strictly approached than at the diffusion time. Nevertheless, the relative error is very small. Note that the SHE model better approaches the kinetic model than the coupled SHE model.

In Ref. [3], it has been shown that the SHE model is surprisingly good in inelastic regimes, at least in steady states simulations. Our aim now is to analyse the behaviour of the SHE and coupled SHE models in inelastic regimes at the diffusion time as well as in steady states. Many questions arise: can the coupled SHE model describe inelastic regimes better than the SHE model ? We recall that the coupled SHE model involves a parameter α which can take any value in an *a priori* limited interval. In our case, α can be chosen so that $\alpha\beta \in (0, 1/2)$. Is the coupled SHE model better than the SHE model for any admissible value of α or only for some values ? Though limited, since restricted to a 1D simulation in a force free case, our study gives a first rough answer to these questions.

First, we give an example of a situation where both models approach well the kinetic model, though in inelastic regimes, and where the coupled SHE model is even better than the SHE model. This simulation is done at $T = T_{diff}$, for different values of β, say, $\beta = 0.1$, $\beta = 0.5$ and $\beta = 1$. Note that the case $\beta = 1$ is the worst possible and corresponds to fully inelastic collisions. We chose α such that the product $\alpha\beta$ remains approximately constant and equal to 0.05. Figures 8, 9 and 10 show the energy and the density for these values. One can see that, for the energy, both SHE models coincide on the left boundary and are not exactly superimposed to the energy curve given by the kinetic model. In the domain and near the right boundary, the approximation gets better and better for the coupled SHE model while the SHE model remains reliable. Such an analysis can be made for the density aswell. In both cases, the coupled SHE model is more accurate than the SHE model far from the left boundary (they are equivalently accurate at the left boundary). Also, it gets better as the inelasticity grows (as $\beta \to 1$) as the comparison of Fig. 8, 9 and 10 reveals it. However, it is remarkable that the SHE model is very good in any case. Even in the case of a fully inelastic scattering ($\beta = 1$), the distribution function at $x = L/2$ is still very well described by the SHE models as can be seen on Fig. 11. On the central hump, the three curves are superimposed. Since there is no elastic scattering, the distribution function is not symmetrized and only one peak appears. In spite of this high dissymmetry, the diffusion models give a good approximation of the peak.

To give a more precise answer to the question of the reliability of the coupled SHE model compared to that of the SHE model, a systematic study of the influence of the couple (α, β) on the relative error between the coupled SHE model and the

kinetic model has been performed at $T = T_{diff}$. Figure 12 presents the relative error (for the density and the energy) in L^1 norm for values of β ranging from 0.01 to 1. It consists in various curves corresponding to the relative error for each value of β, the abscissa being the product $\alpha\beta$ (taken between 0 and 0.01 when possible). The value $\alpha\beta = 0$ corresponds to the uncoupled SHE model.

These graphs show that for any degree of inelasticity for the collisions, *i.e.* for any value of β, the coupled SHE model can become closer to the kinetic model than the SHE model for a convenient value of α. Moreover, the choice of α is not arbitrary since it follows approximately a law of the type $\alpha\beta = 0.045$ as can be read on Fig. 12: the relative errors always reach a minimum for a value of $\alpha\beta$ near 0.045. For $\beta = 0.01$, the constraint $\alpha < 1$ forbids $\alpha\beta$ to reach the value 0.045 so that the relative error reaches its optimum for $\alpha \approx 1$. The coupled SHE model is then better than the SHE model for any value of α. Nevertheless, it has to be noted that the relative error for the SHE model is very small in this case (less than 0.25 %).

A next step is to consider the time evolution of this behaviour. In fact, as it is the case at $T = T_{diff}$ for $\beta = 0.01$, the approximation of the kinetic model by the SHE model is so precise that the coupled SHE model cannot give better results, even though it remains very accurate. In Fig. 13, 14 and 15, we present the comparisons between the SHE models and the kinetic model at $T = 5T_{diff}$ for $\varepsilon = 0.1$ and $\beta = 0.1$, $\beta = 0.5$ and $\beta = 1$. For the coupled SHE model, we consider the optimal value of α as obtained for $T = T_{diff}$, namely, we keep $\alpha\beta$ close to 0.045.

Now, the density aswell as the energy are better approached by the SHE model than by the coupled SHE model, wherever in the domain and for the three regimes ($\beta = 0.1, 0.5, 1$). Consequently, the optimal value of the product $\alpha\beta$, for which the coupled SHE model gave the best approximation, does not remain optimal for any time. In particular, the steady state is not described the best by the coupled SHE model for this value. Figure 16 gives a precise meaning to this remark. Indeed, it represents the time evolution of the relative error (in L^1 norm) for the density and for the energy between the coupled SHE model and the kinetic model. The comparison is made for $\varepsilon = 0.1$, $\beta = 0.3$ and we chose α such that $\alpha\beta = 0.05$ (the optimal value for $T = T_{diff}$). Let us first consider the relative error for the density. The relative error is very high at the beginning for both models (which is not surprising since these models are theoretically relevant for diffusion regimes and not for short times), though higher for the coupled SHE model than for the

SHE model. The error decreases and reaches a minimum for both models (around $T = 0.3T_{diff}$ for the SHE model, near T_{diff} for the coupled SHE model). Then the evolution is different since the error for the coupled SHE model grows until $T = 5T_{diff}$ while the error for the SHE model first grows until $T \approx 0.7T_{diff}$ and then decreases again. Note that, from $T = 0.2T_{diff}$ to $T = 5T_{diff}$, the SHE model keeps very accurate since the relative error remains smaller than 1 %. The relative error for the coupled SHE model remains less than 2 % for $T \in (0.3T_{diff},\ 5T_{diff})$ and, at $T = T_{diff}$, it is twice as accurate as the SHE model. For the energy, the evolution is qualitatively the same, but the error is smaller for both models.

4.2 The transient regime

In this section simulations for times lower than T_{diff} are given. We present comparisons for an intermediate small time, $T = 0.05T_{diff}$. The parameter α in the coupled SHE model is chosen such that $\alpha\beta$ corresponds to the optimal value at T_{diff}. In fact, the simulations show that there is no such an optimal value for small enough times (see the discussion in section 4.1). We present a simulation for $\beta = 0.3$, a moderately inelastic regime. For this value of β, Fig. 17 presents the energy and density curves. The coincidence of the SHE models with the kinetic equation is obviously not as good as at $T = T_{diff}$, but the macroscopic models remain very close to the kinetic model. Moreover, the coupled SHE model is less accurate than the SHE model in this case as could be expected according to Fig. 16 which shows that, for small times, the relative error between the coupled SHE model and the kinetic model is higher (for the density as well as for the energy) than the relative error between the SHE and kinetic models.

5 Conclusion

In this paper, the results of numerical simulations for the SHE and the coupled SHE models have been presented. The simulations were carried out in an unstationary, force free case.

The presented results mainly concern macroscopic quantities such as the density and the energy. Meanwhile, we also established that we can recover much information on the distribution function through the SHE models.

To the questions raised by the differences between the SHE and coupled SHE models, the answers given in this paper must be considered as partial and temporary for many reasons among which the fact that the test case considered is very simple and cannot claim to give more than preliminary indications for future investigations. In particular, for the time being, no unstationary simulation taking a force field into account has been performed and we can hardly imagine what differences the extension to multidimensional cases may induce.

Nevertheless, the following facts are of some interest. First, our simulations show that both the coupled and the uncoupled SHE models seem to be highly reliable for scatterings going to quasi-elastic to fully inelastic. On the other hand, the reliability is important not only for times greater than the diffusion time, but also in the transient regime, even for rather small times (of the order of $0.05T_{diff}$), which is quite surprising for a diffusion model.

In some cases, in particular at the diffusion time and for smaller times, the coupled SHE model gives a better approximation of the kinetic model than the classical SHE model. Moreover, the influence of the value of the coupling parameter α follows a simple rule, at least at the diffusion time.

The results presented in this paper are encouraging: the coupled and uncoupled SHE models proved to be very relevant to describe transport phenomena not only at a diffusion scale. Nevertheless, many questions remain open. In particular, future work will be dedicated to the extension to non zero force fields.

Aknowledgment

We are grateful to Pierre Degond who suggested this study and provided us with very helpful comments.

References

[1] A. Gnudi, D. Ventura, G. Baccarani and F. Odeh, Two-dimensional MOSFET simulation by means of a multidimensional spherical harmonic expansion of the Boltzmann transport equation, *Solid State Electron.* **36** 575-581 (1993).

[2] P. Degond, An infinite system of diffusion equations arising in transport theory: the coupled Spherical Harmonics Expansion model, *Math. Models Methods Appl. Sci.* **11** (5) 903-932 (2001).

[3] P. Degond, V. Latocha, L. Garrigues and J.P. Boeuf, Electron transport in stationary plasma thrusters, *Transp. Th. Stat. Phys.* **27** 203-221 (1998).

[4] T. Goudon and A. Mellet, Discrete version of the SHE asymptotics: Multigroup neutron transport equations, *J. Math. Phys.* **43** (6) 3232-3260 (2002).

[5] J.P. Bourgade, On spherical harmonics expansion type models for electron-phonon collisions, *Math. Methods Appl. Sci.* **26** (3) 247-271 (2003).

[6] P. Degond and C. Schmeiser, Macroscopic models for semiconductor heterostructures, *J. Math. Phys.* **39** (9) 4634-4663 (1998).

[7] E. Sonnendrücker, J. Roche, P. Bertrand and A. Ghizzo, The Semi-Lagrangian Method for the Numerical Resolution of the Vlasov Equation, *J. Comp. Phys.* **149** 201-220 (1999).

[8] F. Filbet, *Contribution à l'analyse et à la simulation numérique de l'équation de Vlasov*, PhD Thesis, Université Henri Poincaré-Nancy I.

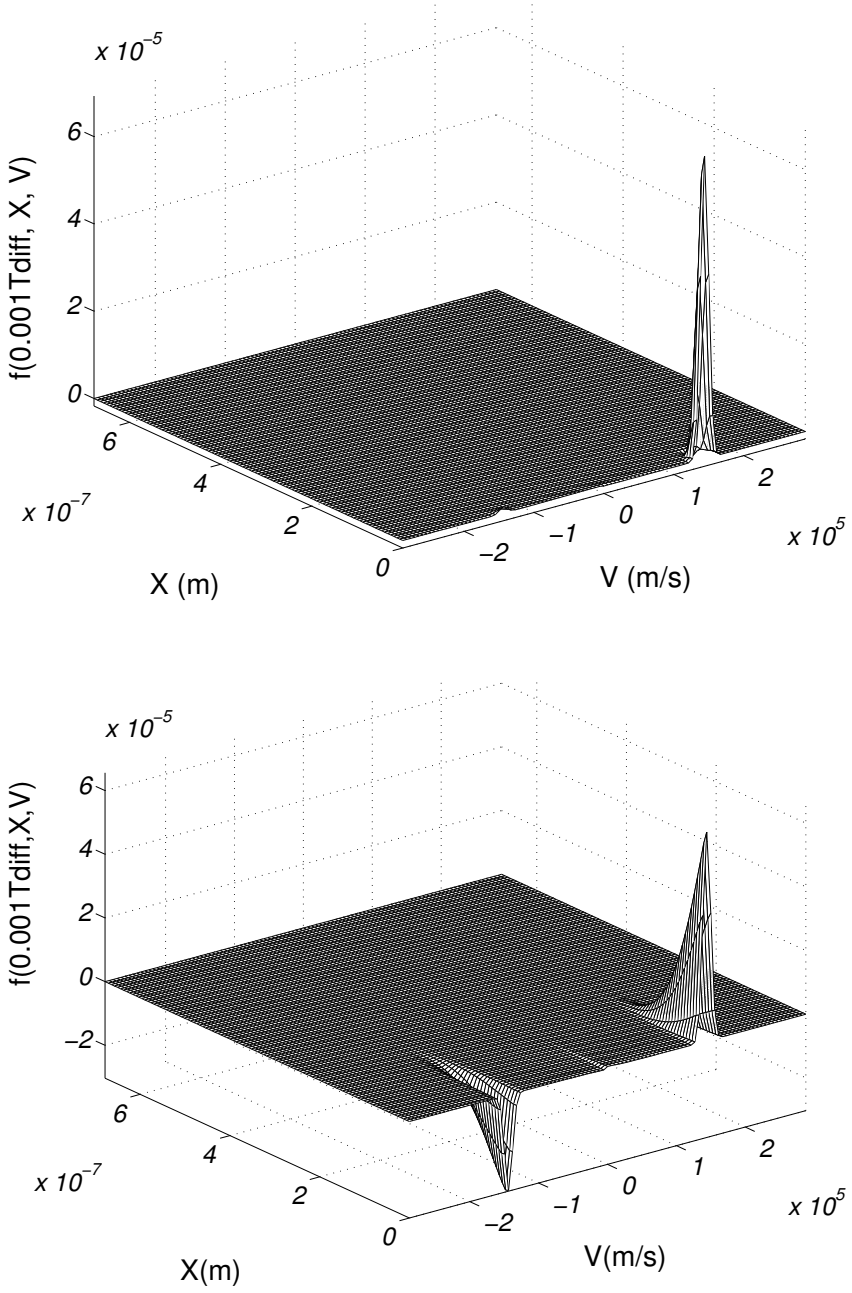

Figure 1: Distribution function at $T = 0.001T_{diff}$ for the Kinetic (top) and the Coupled SHE (bottom) models

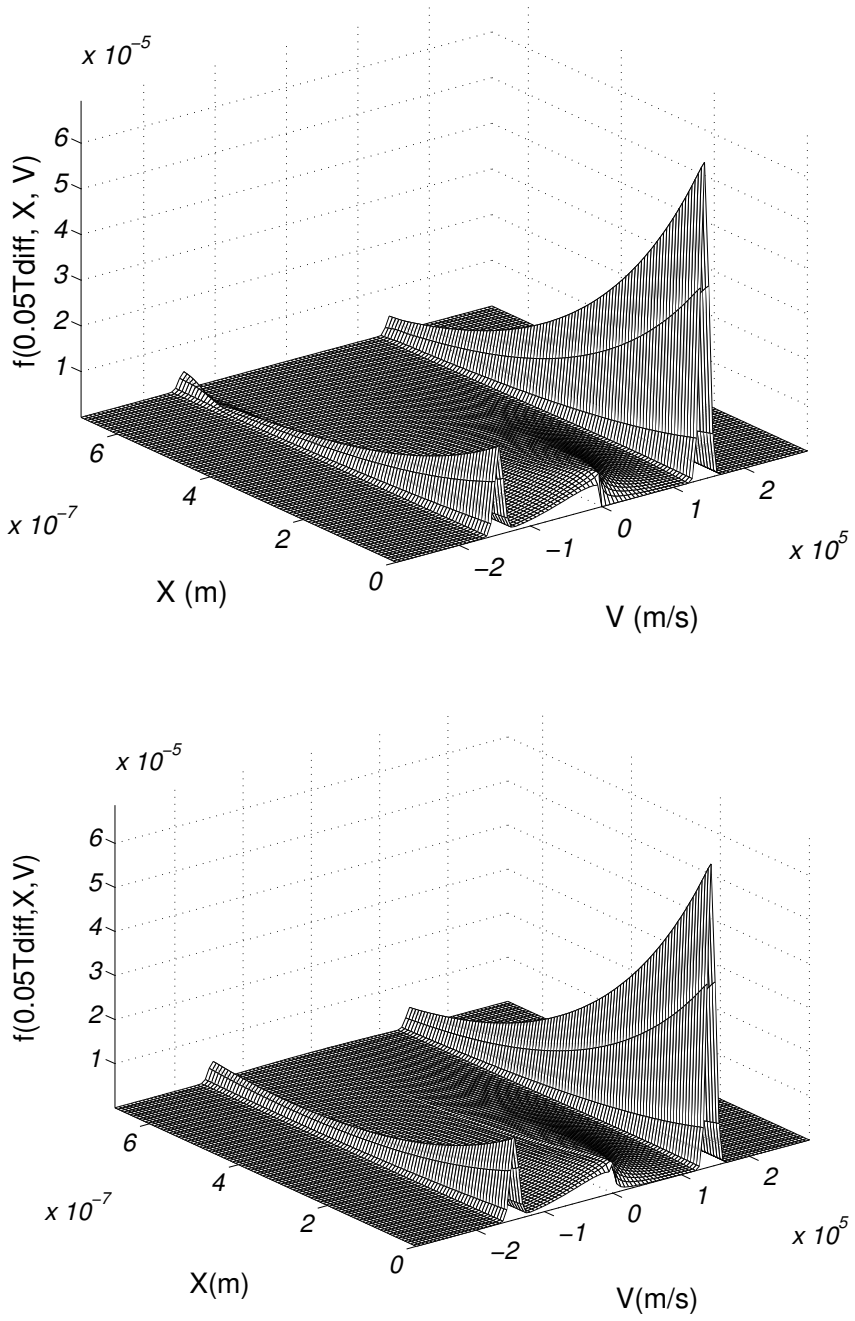

Figure 2: Distribution function at $T = 0.05T_{diff}$ for the Kinetic (top) and the Coupled SHE (bottom) models

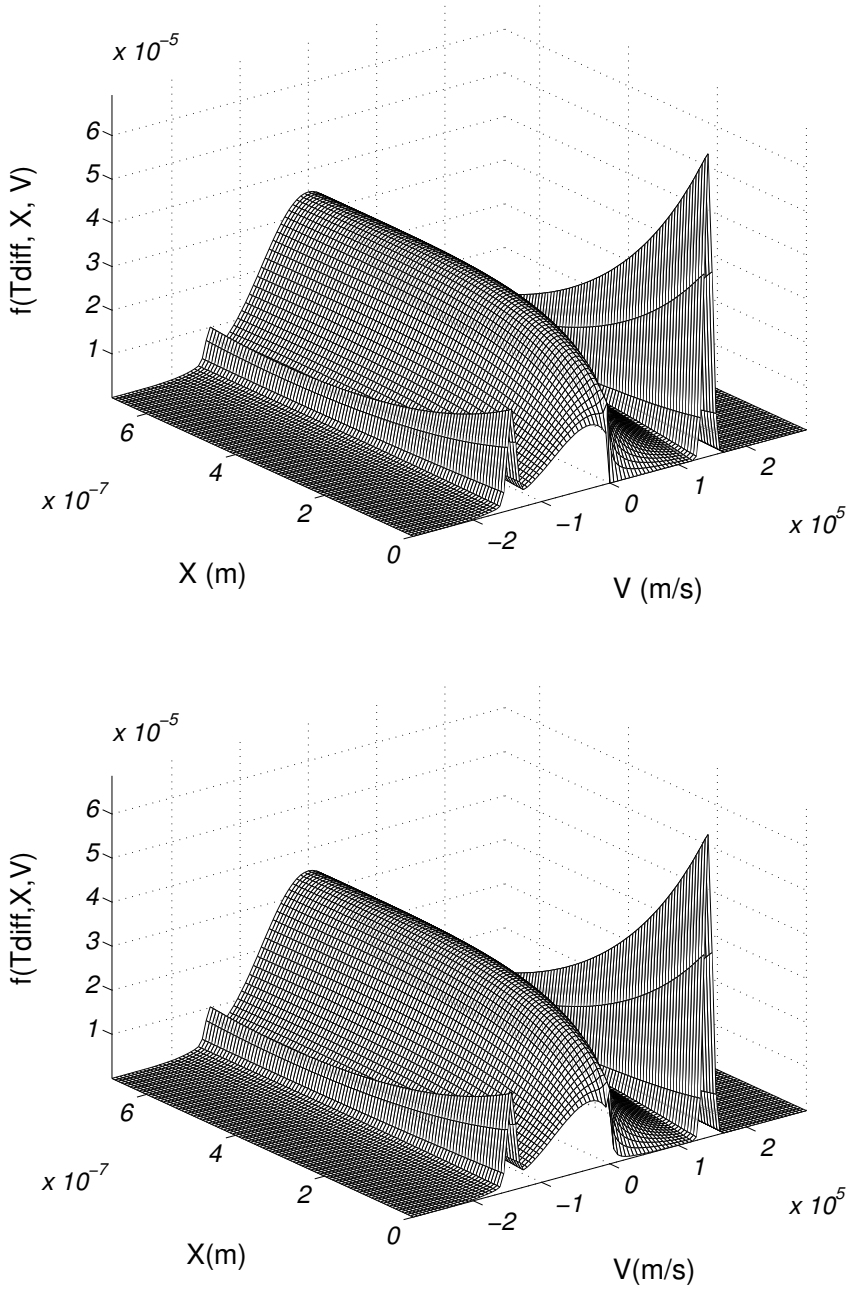

Figure 3: Distribution function at $T = T_{diff}$ for the Kinetic (top) and the Coupled SHE (bottom) models

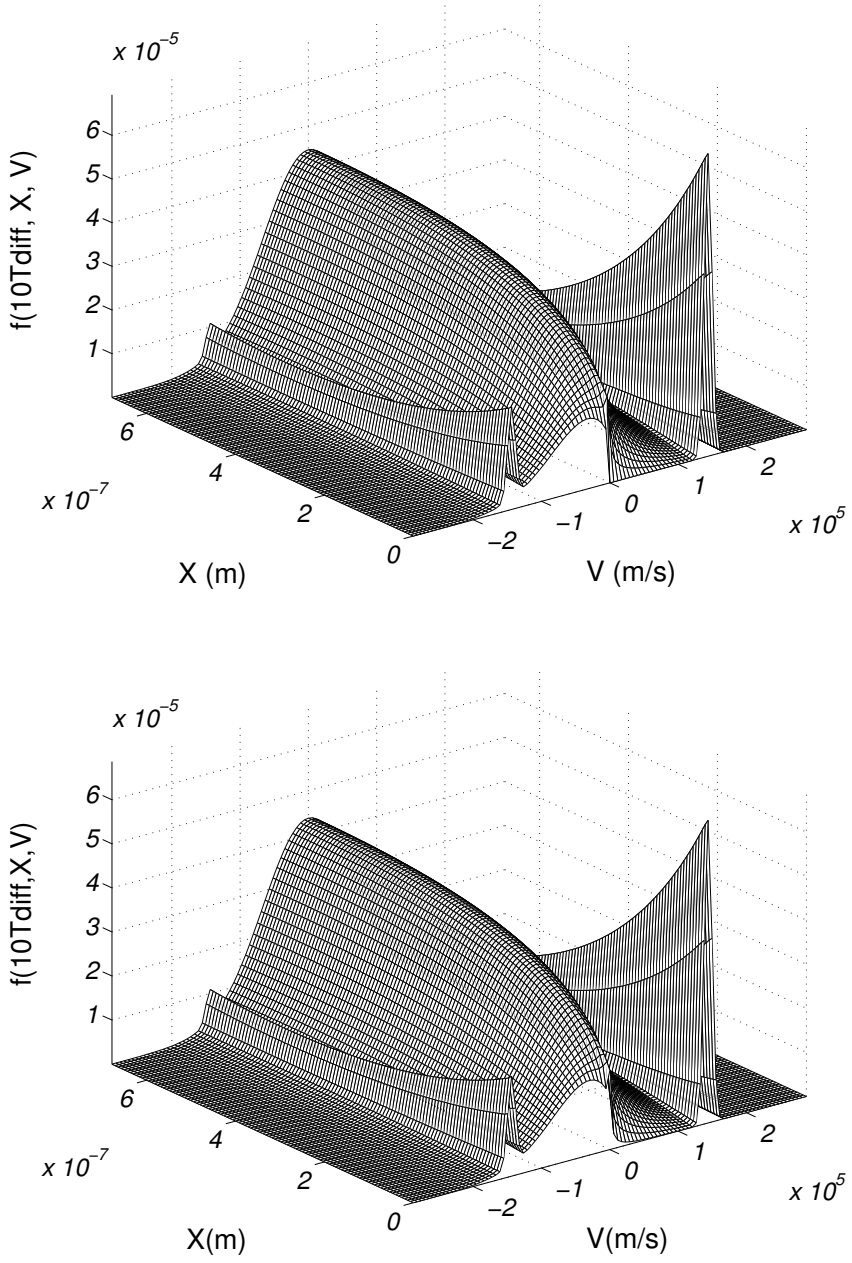

Figure 4: Distribution function at $T = 10T_{diff}$ for the Kinetic (top) and the Coupled SHE (bottom) models

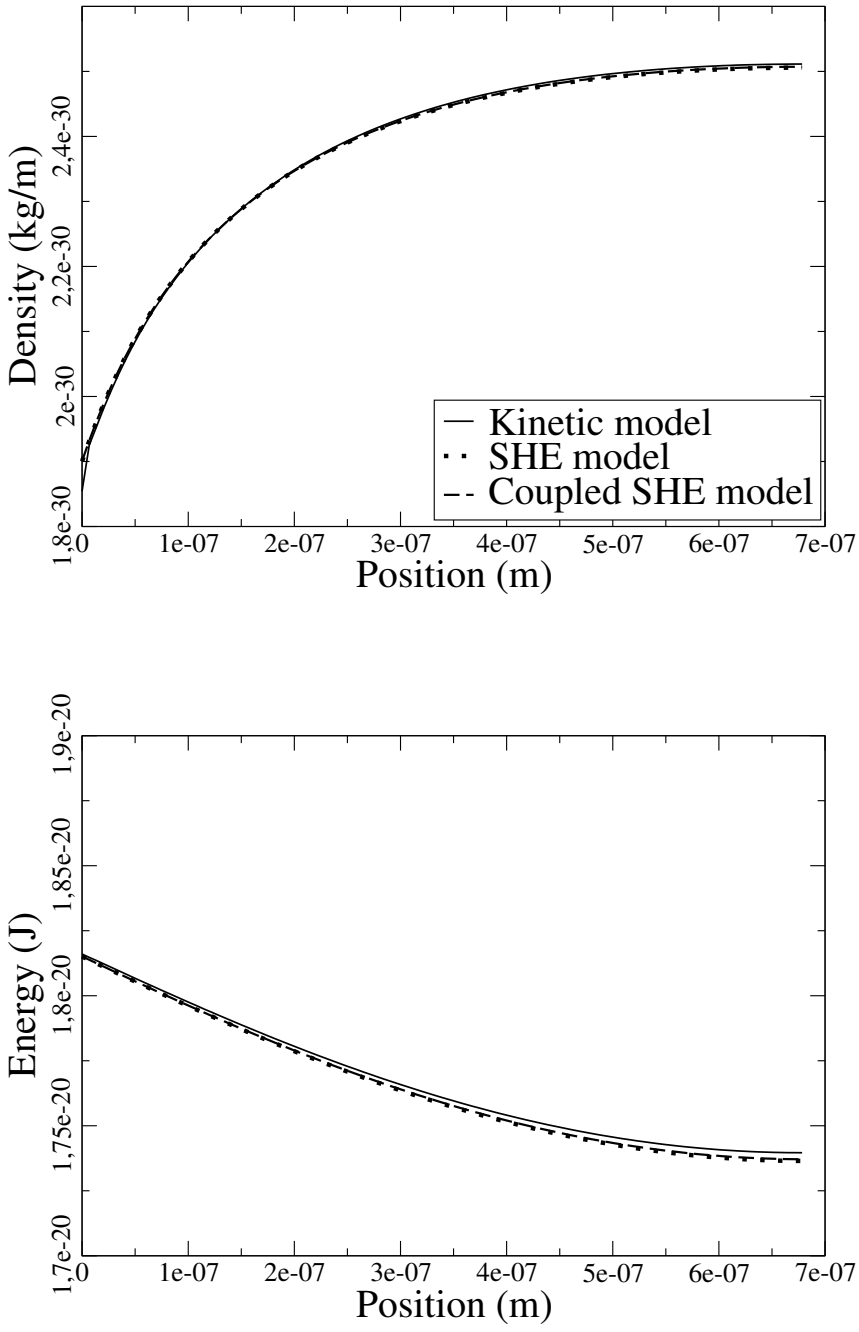

Figure 5: Density (top) and energy (bottom) at $T = T_{diff}$, for $\varepsilon = 0.1$, $\beta = 0.01$, $\alpha = 0.5$: comparison between the kinetic, SHE and coupled SHE models.

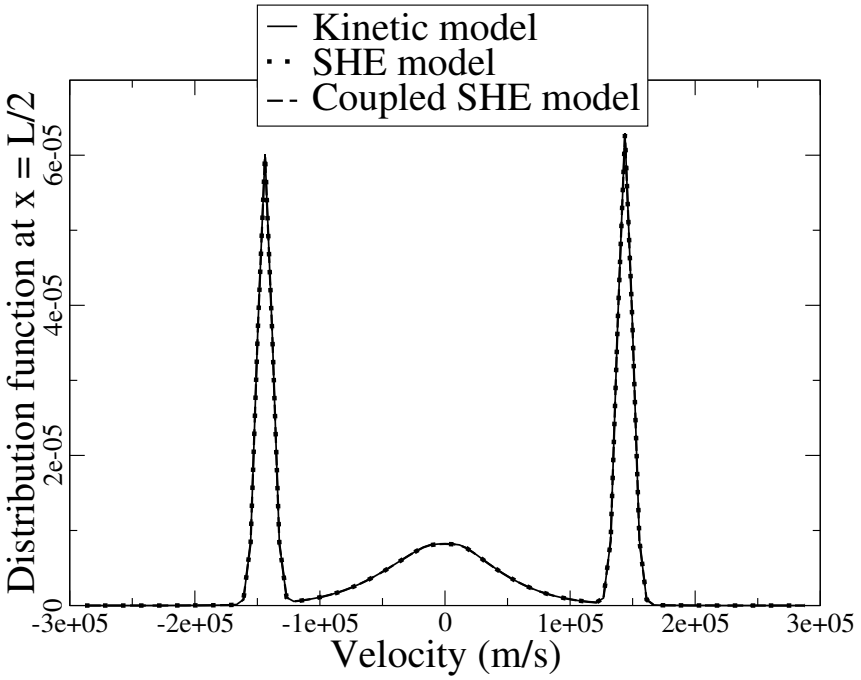

Figure 6: Distribution function at $T = T_{diff}$, $x = L/2$, for $\varepsilon = 0.1$, $\beta = 0.01$, $\alpha = 0.5$: comparison between the kinetic, SHE and coupled SHE models.

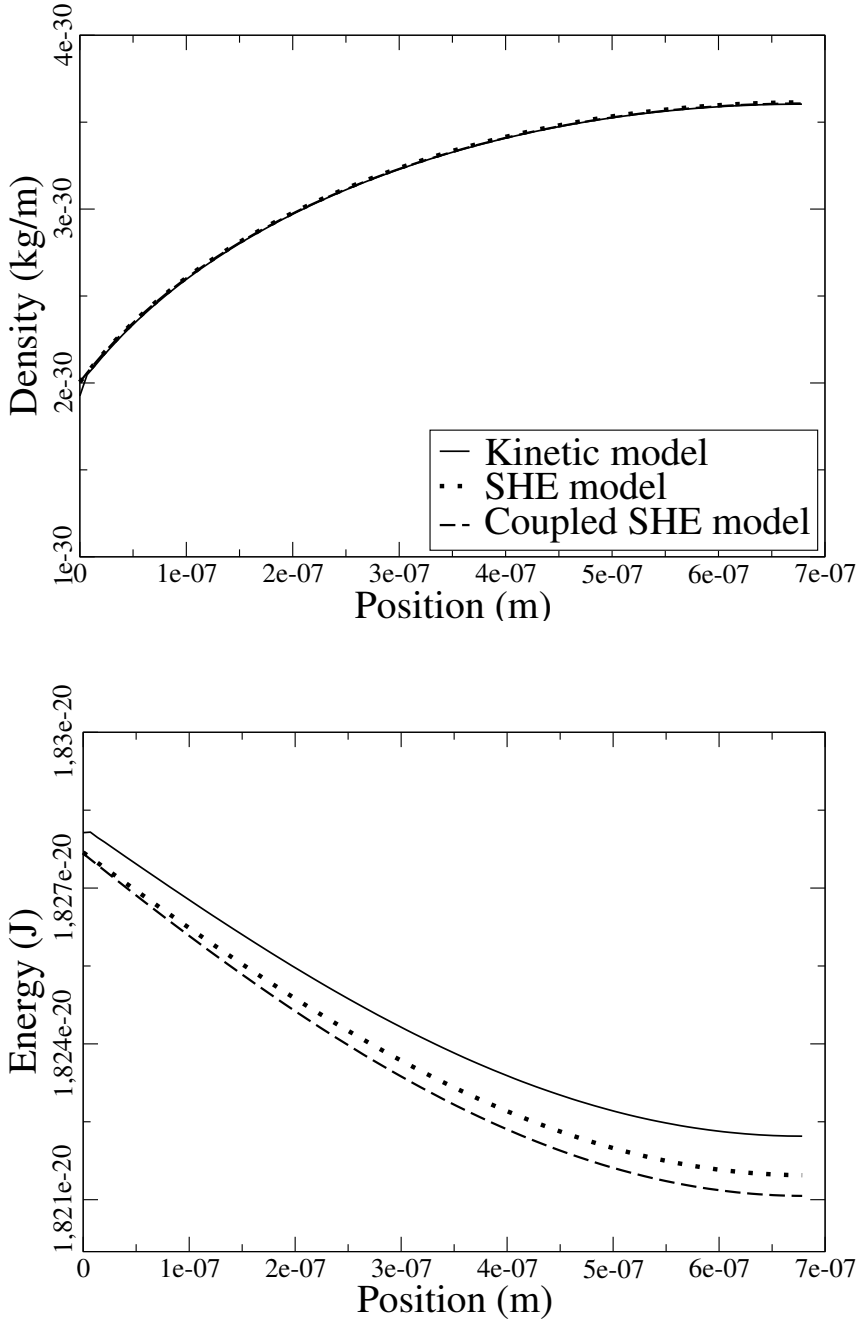

Figure 7: Density (top) and energy (bottom) at $T = 5T_{diff}$, for $\varepsilon = 0.1$, $\beta = 0.01$, $\alpha = 0.5$: comparison between the kinetic, SHE and coupled SHE models.

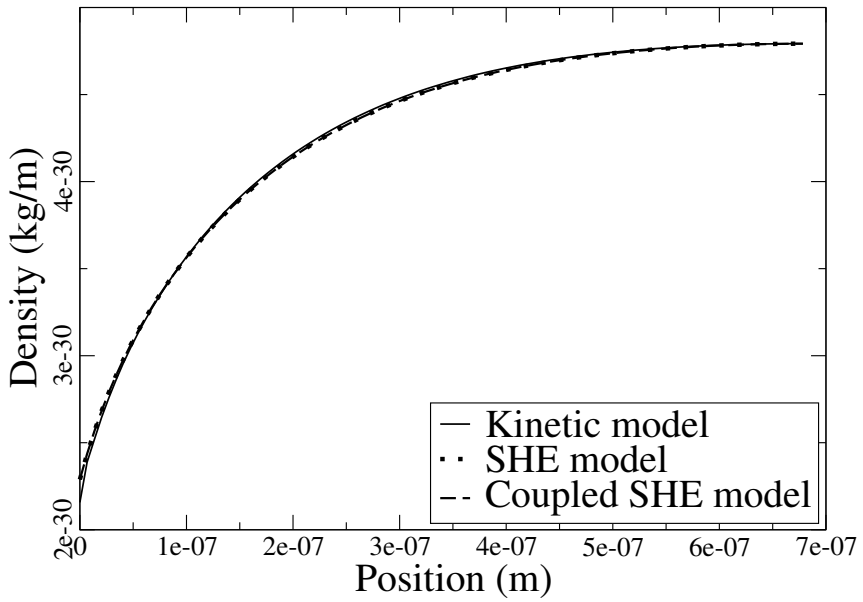

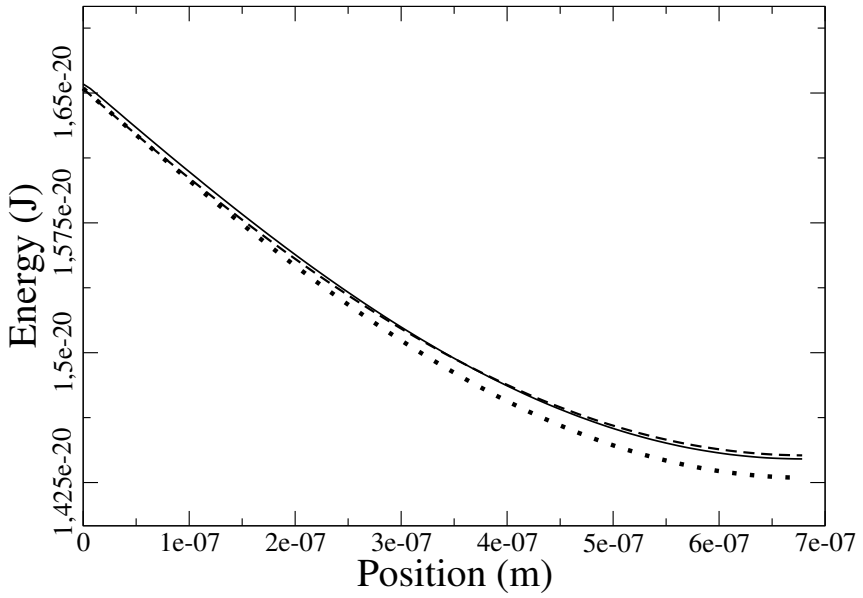

Figure 8: Density (top) and energy (bottom) at $T = T_{diff}$, for $\varepsilon = 0.1$, $\beta = 0.1$, $\alpha = 0.4$: comparison between the kinetic, SHE and coupled SHE models.

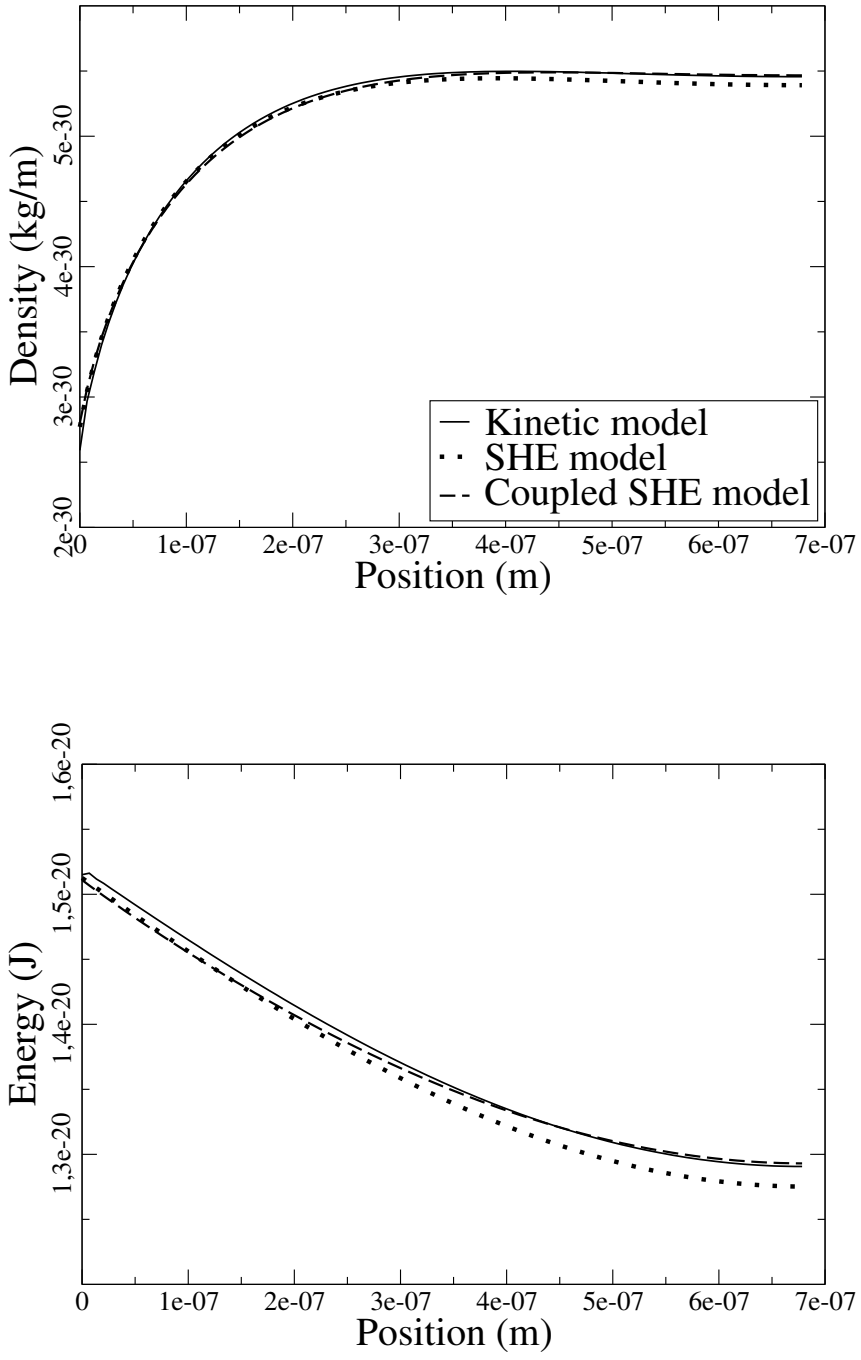

Figure 9: Density (top) and energy (bottom) at $T = T_{diff}$, for $\varepsilon = 0.1$, $\beta = 0.5$, $\alpha = 0.1$: comparison between the kinetic, SHE and coupled SHE models.

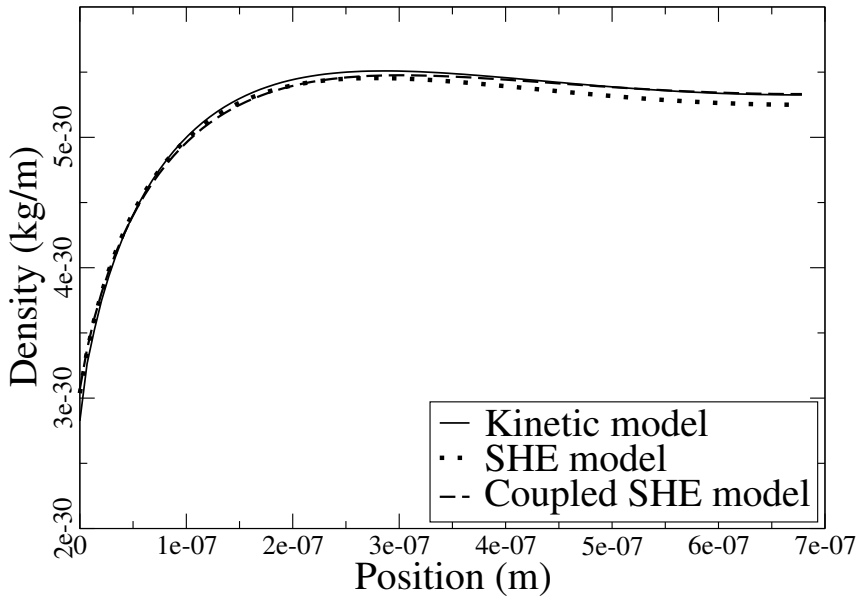

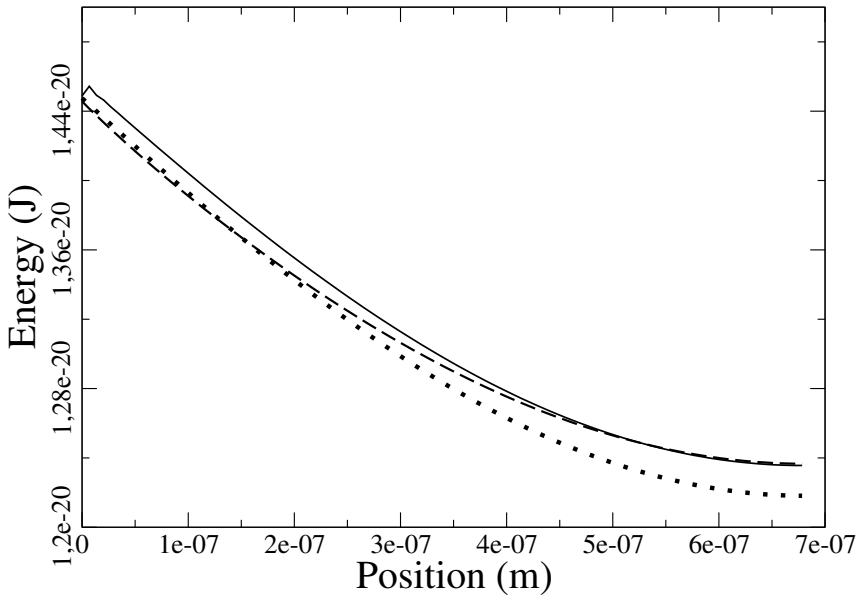

Figure 10: Density (top) and energy (bottom) at $T = T_{diff}$, for $\varepsilon = 0.1$, $\beta = 1$, $\alpha = 0.05$: comparison between the kinetic, SHE and coupled SHE models.

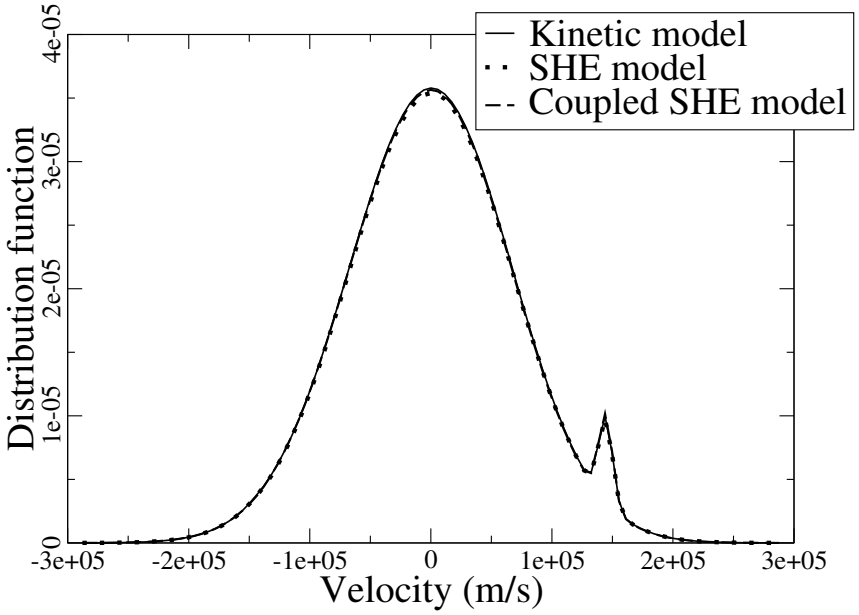

Figure 11: Distribution function at $T = T_{diff}$, $x = L/2$, for $\varepsilon = 0.1$, $\beta = 1$, $\alpha = 0.05$: comparison between the kinetic, SHE and coupled SHE models.

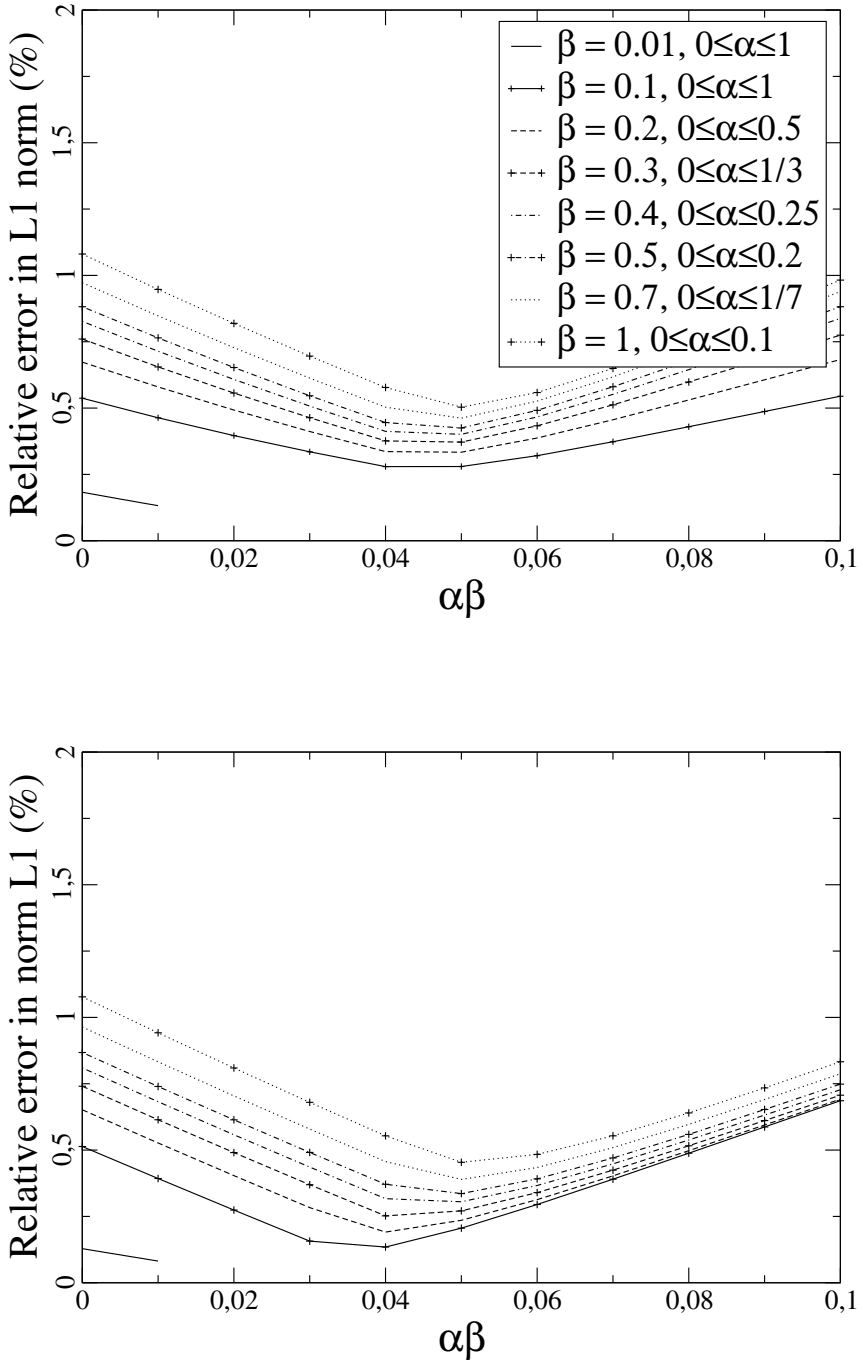

Figure 12: Relative errors in L^1 norm for the density (top) and the energy (bottom) at $T = T_{diff}$, for $\varepsilon = 0.1$: comparison between the kinetic, SHE ($\alpha\beta = 0$) and coupled SHE ($\alpha\beta \neq 0$) models.

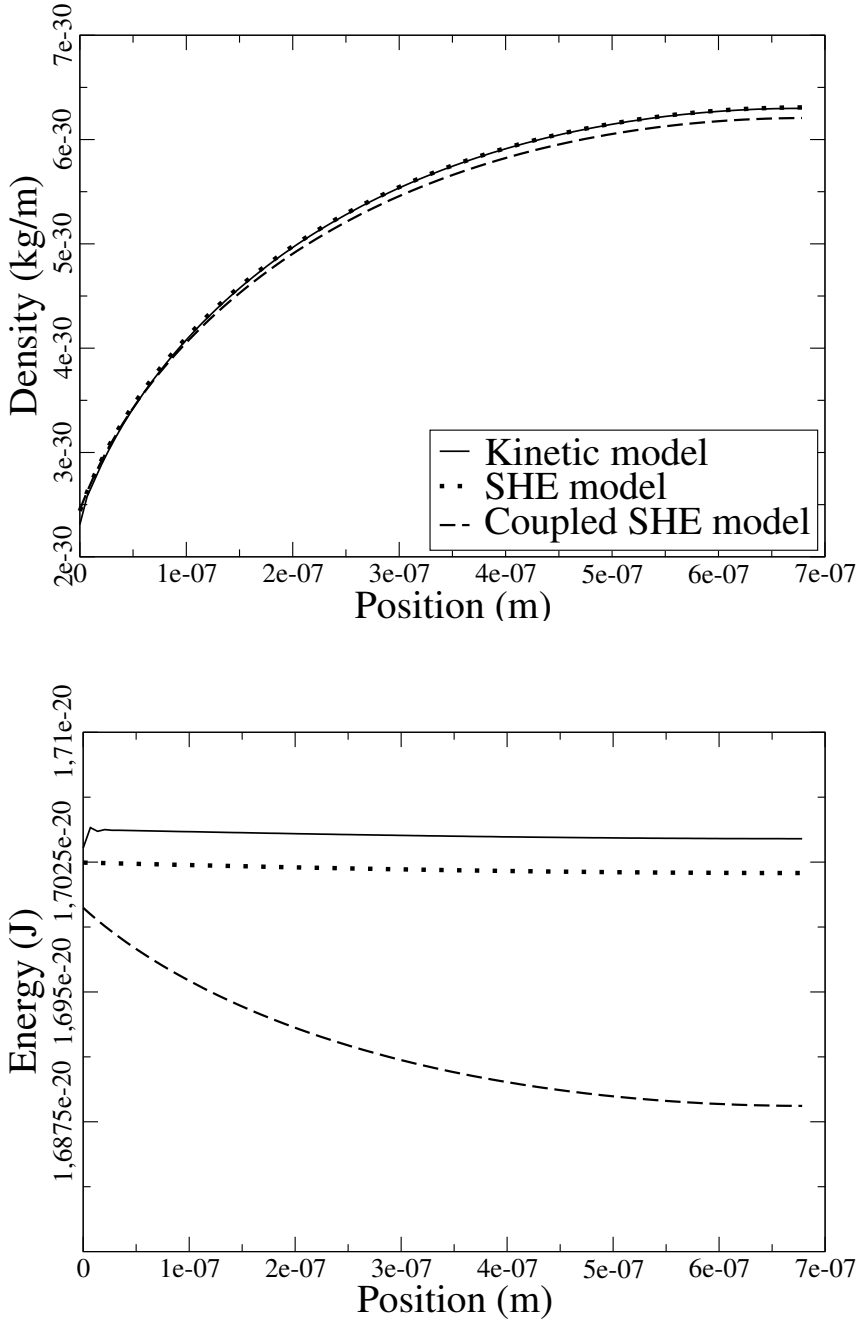

Figure 13: Density (top) and energy (bottom) at $T = 5T_{diff}$, for $\varepsilon = 0.1$, $\beta = 0.1$, $\alpha = 0.4$: comparison between the kinetic, SHE and coupled SHE models.

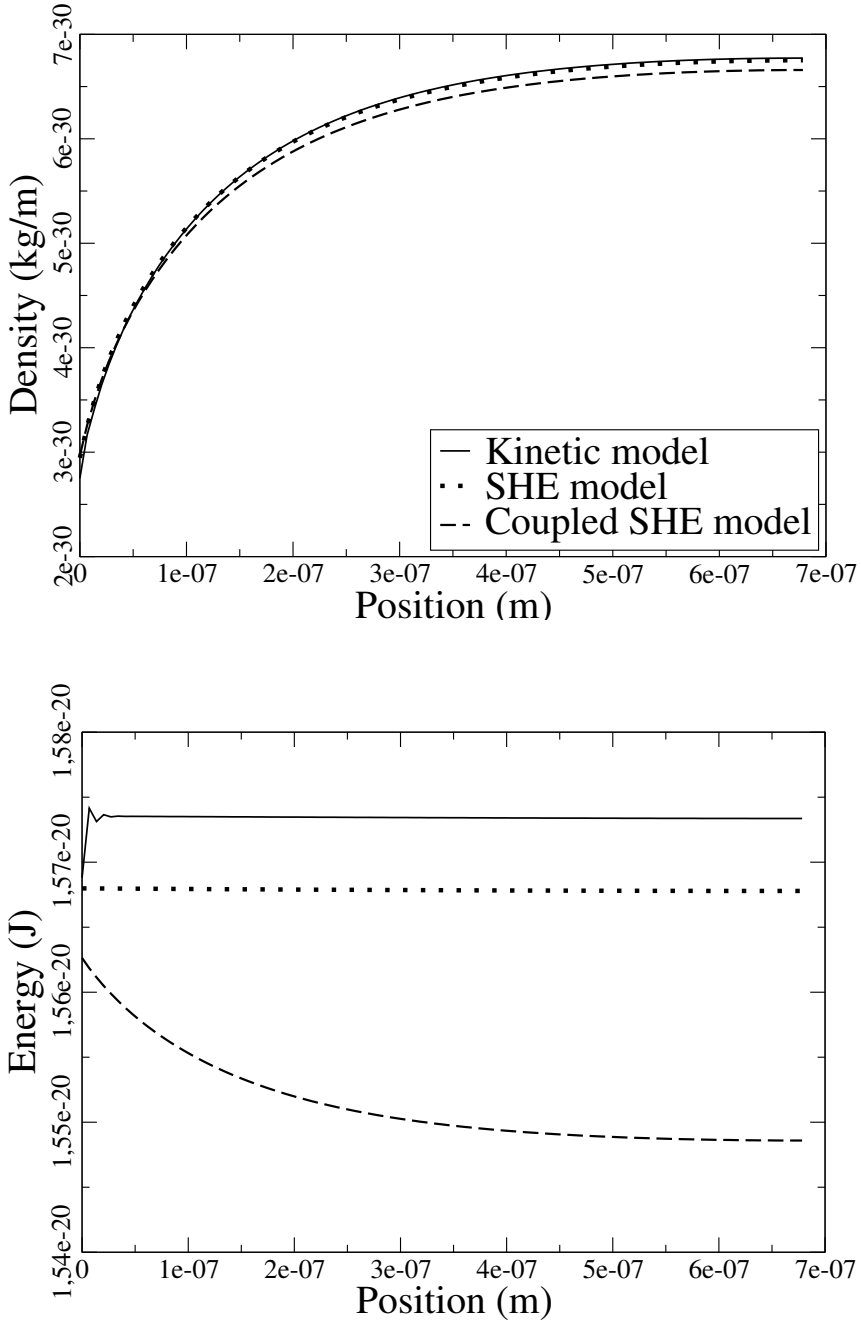

Figure 14: Density (top) and energy (bottom) at $T = 5T_{diff}$, for $\varepsilon = 0.1$, $\beta = 0.5$, $\alpha = 0.1$: comparison between the kinetic, SHE and coupled SHE models.

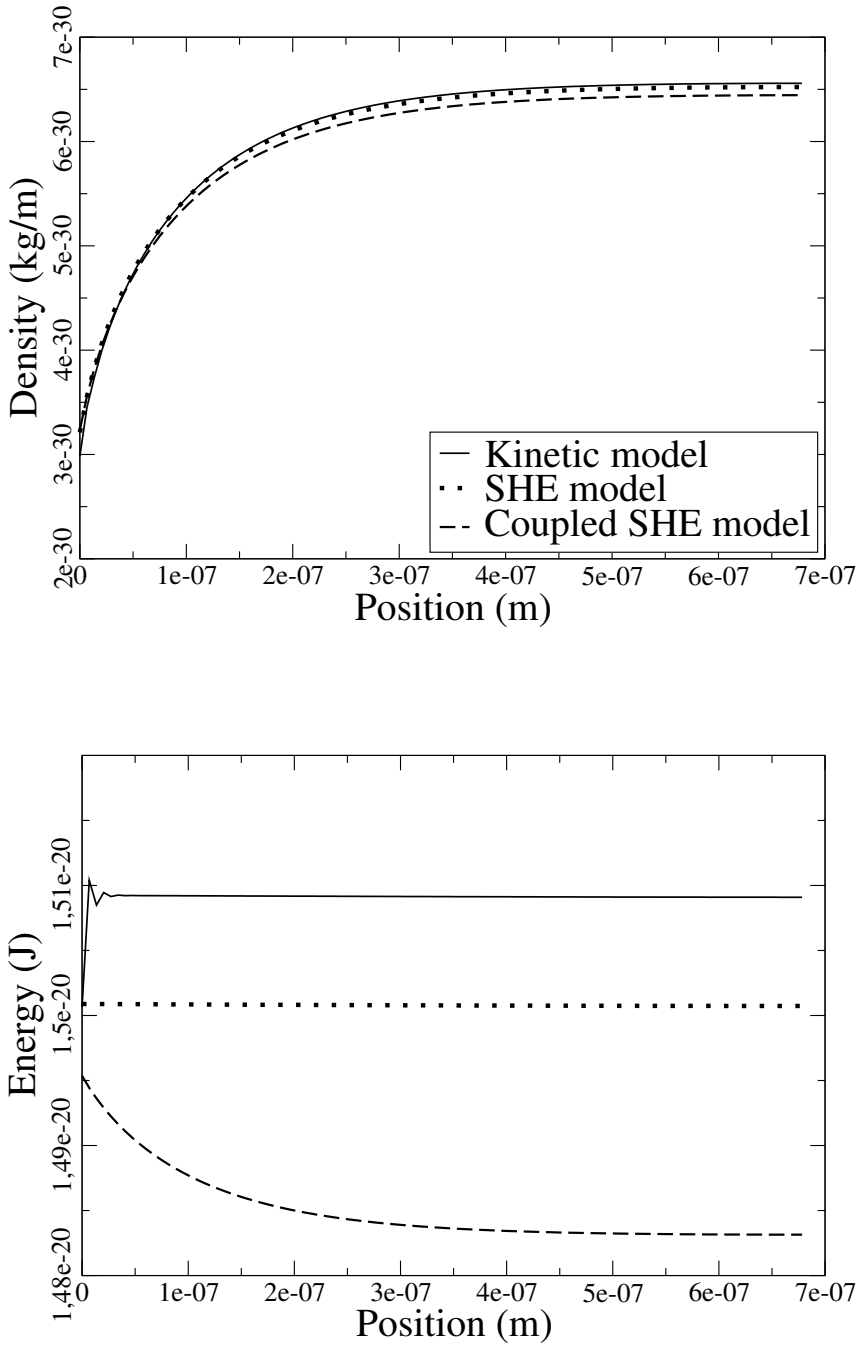

Figure 15: Density (top) and energy (bottom) at $T = 5T_{diff}$, for $\varepsilon = 0.1$, $\beta = 1$, $\alpha = 0.05$: comparison between the kinetic, SHE and coupled SHE models.

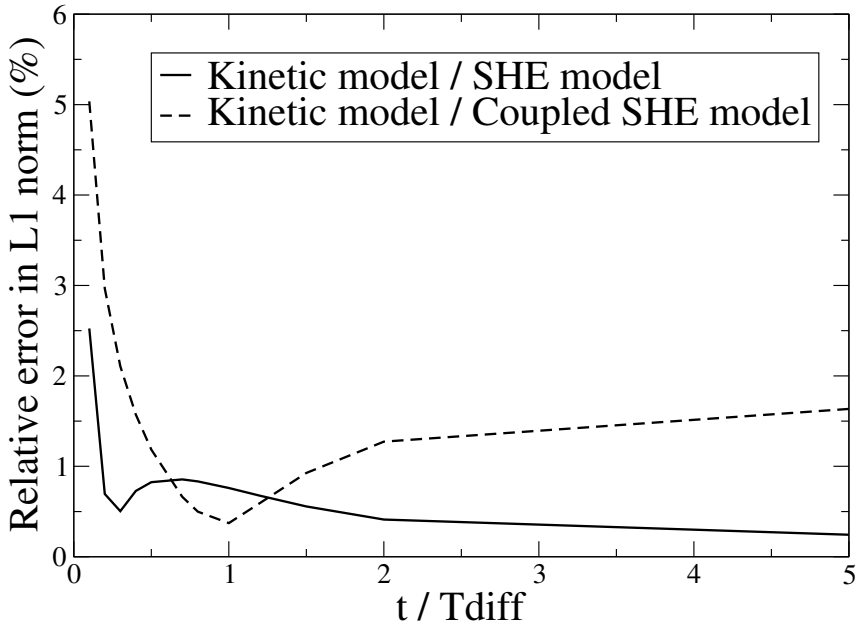

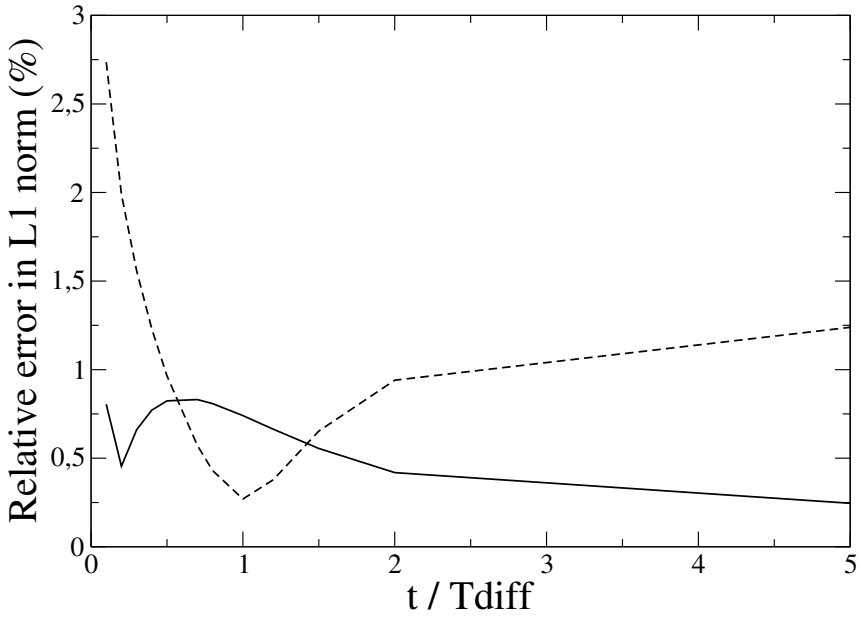

Figure 16: Time evolution of the relative error in L^1 norm for the density (top) and the energy (bottom) for $\varepsilon = 0.1$, $\beta = 0.3$, $\alpha = 0.166$: comparison between the kinetic and the SHE models.

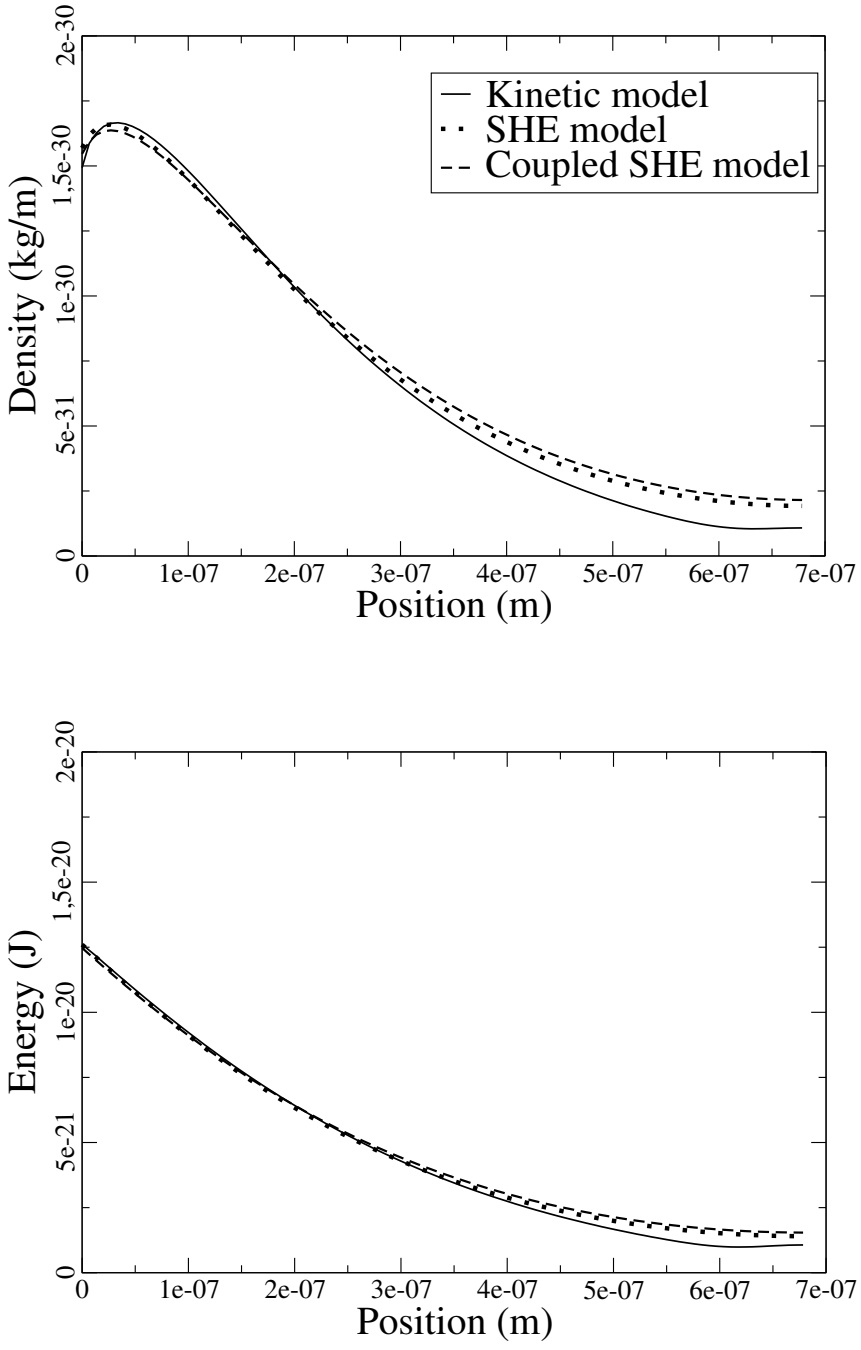

Figure 17: Density (top) and energy (bottom) at $T = 0.05T_{diff}$, for $\varepsilon = 0.1$, $\beta = 0.3$, $\alpha = 0.166$: comparison between the kinetic, SHE and coupled SHE models.